



MTRNet++: One-stage Mask-based Scene Text Eraser

Osman Tursun^{a,**}, Simon Denman^a, Rui Zeng^{a,b}, Sabesan Sivapalan^a, Sridha Sridharan^a, Clinton Fookes^a

^aImage and Video Lab, Queensland University of Technology, Queensland, Australia

^bAustralian Centre for Robotic Vision, Monash University, Victoria, Australia

ABSTRACT

A precise, controllable, interpretable and easily trainable text removal approach is necessary for both user-specific and large-scale text removal applications. To achieve this, we propose a one-stage mask-based text inpainting network, MTRNet++. It has a novel architecture that includes mask-refine, coarse-inpainting and fine-inpainting branches, and attention blocks. With this architecture, MTRNet++ can remove text either with or without an external mask. It achieves state-of-the-art results on both the Oxford and SCUT datasets without using external ground-truth masks. The results of ablation studies demonstrate that the proposed multi-branch architecture with attention blocks is effective and essential. It also demonstrates controllability and interpretability.

© 2022 Elsevier Ltd. All rights reserved.

1. Introduction

Text removal is the task of inpainting text regions in scenes with semantically correct backgrounds. It is useful for privacy protection, image/video editing, and image retrieval (Tursun et al., 2018). Recent studies with advanced deep learning models (Zhang et al., 2018; Tursun et al., 2019; Nakamura et al., 2017) explore removing text from real world scenes. Previously, text removal with traditional methods has only been effective for text in fixed positions with a uniform background from digital-born content.

Text removal is a challenging task as it inherits the challenges of both text-detection and inpainting tasks. Zhang et al. (2018) claims that text removal requires stroke-level text localization, which is a harder and less studied topic compared to bounding-box-level scene text detection (Gupta et al., 2016). On the other hand, realistic inpainting requires replacing/filling unwanted objects in scenes with perceptually plausible content. Deep learning approaches generate perceptually plausible content by learning the distribution of training data. Text can be placed in any region or on any object, and as such a text inpainting model is required to learn a wide range of distributions, exacerbating the challenge.

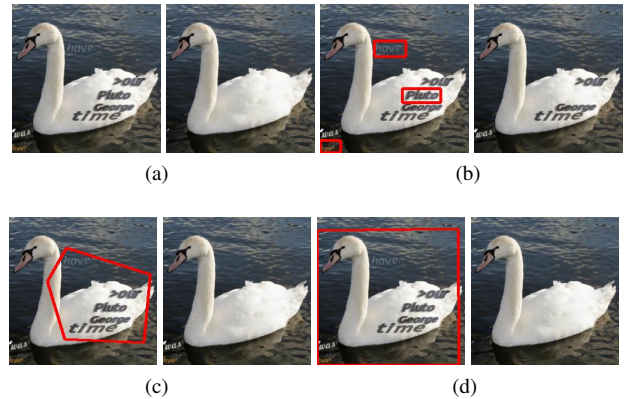


Fig. 1: MTRNet++ is a one-stage text removal approach which removes text either with or without a mask. In the without mask case, MTRNet++ will remove all text in a scene as shown in Fig. 1a. While with a mask, MTRNet++ is able to only remove text under the masked region as shown in Figs. 1b-d. Note that masked regions are labelled with polygons using red outlines.

Recent text removal studies are based around two main paradigms: one-stage and two-stage methods. The one-stage approach uses an end-to-end model, which is free of auxiliary inputs; however, its generality, flexibility and interpretability are limited. EnsNet (Zhang et al., 2018) is the state-of-the-art one-stage text removal method. It removes all text that is written in scripts on which it was trained. Although it supports selective text removal with some extra steps (cropping or

^{**}Corresponding author

^{e-mail:} w.tuerxun@qut.edu.au (Osman Tursun)

^{***} Under CVIU review. ^{***}

overlapping), this introduces new issues such as color discontinuities or loss of context. Moreover, it lacks interpretability that makes fixing failure cases troublesome. Finally, yet importantly, we found that a one-stage approach without an explicit text localisation mechanism fails to converge on a large-scale dataset within a few epochs. For example, Pix2Pix (Isola et al., 2017) and EnsNet do not converge on a large-scale dataset with the same amount of training as their counterparts did according to the results reported in MTRNet (Tursun et al., 2019) and this work.

The two-stage approach decomposes the text removal task into text detection and text inpainting sub-problems. Text detection can be manual or automatic. MTRNet (Tursun et al., 2019), for example, is a representative two-stage approach with a deep neural network. The main advantage of a two-stage approach is that it has an awareness of the text regions that require inpainting. With explicit text regions, it gains generality and controllability. Two stage approaches can be effortlessly adapted to remove text in various scripts, and are able to remove or keep text based on selection. Such methods have strong interpretability as well; for example it is easier to understand if failure cases are caused by inaccurate detection or poor inpainting. Despite the promise of two-stage methods, they are limited in that they rely on a text localisation front-end. Compared to a one-stage approach, two stage approaches are inefficient and have a complex training process as at least two networks need to be trained.

In this work, we propose a one-stage text removal approach, MTRNet++. It can remove text either with a mask as per MTRNet, or without a mask as per EnsNet as shown in Fig. 1. It inherits the idea of MTRNet of using a text region mask as an auxiliary input. However, the network has a different architecture to MTRNet, and is composed of *mask-refine*, *coarse-inpainting*, and *fine-inpainting* branches. The mask-refine and coarse-inpainting branches generate intermediate results, while the fine-inpainting branch generates the final refined results. Moreover, compared to MTRNet, it can remove text under very coarse masks as shown in Figs. 1c and 1d.

The mask-refine branch is designed to refine a coarse mask into an accurate pixel-level mask. The mask-refining branch is introduced for the following reasons: (1) To remove text as EnsNet does without requiring third-party text-localisation information, but also to allow utilisation of third-party information as done by MTRNet. (2) To provide interpretability, flexibility and a generalisation ability. (3) To provide attention scores to the coarse-inpainting branch. (4) To speed up the convergence of the network on a large-scale dataset.

The coarse-inpainting branch is a parallel branch to the mask-refine branch, which performs a coarse inpainting using the coarse mask. The coarse-to-fine framework has been shown to be beneficial for realistic inpainting (Yu et al., 2018b; Ma et al., 2019), and the coarse-branch is guided by the attention scores generated by the attention blocks that map intermediate features of the mask-refine branch to weights.

The fine-inpainting branch is introduced for refining the results of the coarse-inpainting branch with precise masks from the mask-refine branch. The coarse results are blurry and lack

details. The fine-inpainting branch increases inpainting quality. In this work, for efficiency, a light sub-network is used as the fine-inpainting branch.

In summary, our contributions are as follows:

- We propose a novel one-stage architecture for text removal. With this architecture, MTRNet++ is free from external text localisation methods, yet can also leverage external information.
- MTRNet++ achieves state-of-the-art quantitative and qualitative results both on Oxford (Gupta et al., 2016) and SCUT (Zhang et al., 2018) datasets without external masks. Ablation studies shows the proposed architecture and its components play important roles.
- MTRNet++ is a fully end-to-end trainable network and is easily trainable. It converges on large-scale datasets within an epoch. It also demonstrates controllability and interpretability.

We also introduce other incremental modifications regarding training losses, training strategy and the discriminator, which will be discussed in Section 3.

The rest of the paper is organised as follows. The next section presents related literature. Section 3 illustrates the proposed network architecture (generator and discriminator), training losses and training strategy. Section 4 presents experiments, ablation studies and analysis. Finally, we provide a brief summarisation of our work in Section 5.

2. Literature

Text removal is a special case of image inpainting, which usually requires the assistance of a text-detection method for text localization. Early text removal approaches (Khodadadi and Behrad, 2012; Wagh and Patil, 2015; Tursun et al., 2018) are two-stage methods based on either traditional text detection or inpainting approaches. With the advance of deep learning, many classical problems including image inpainting are solved in a single stage using a deep encoder-decoder neural network (Mao et al., 2016). By being fed numerous examples, the neural network learns to map the input to the text-free ground-truth. Nakamura et al. (2017) proposed the first one-stage text removal approach, which is a patch-based skip-connected auto-encoder. They trained the network by providing patches with text and patches without text. Inpainting results of the early one-stage approach are blurry and lack detail, as networks are trained with only pixel intensity-based losses.

Later works improve inpainting via new losses generated from a neural network (Yang et al., 2017; Liu et al., 2018; Isola et al., 2017; Iizuka et al., 2017), such as content and style losses which are calculated using classification networks pre-trained on image-net. Adversarial losses obtained from a generative adversarial network (GAN) Yu et al. (2018b) have also shown promise for inpainting. Recent works (Jo and Park, 2019; Nazari et al., 2019) show that using both a pre-trained classification network and a newly trained discriminator for image inpainting

is beneficial. Zhang et al. (2018) trained a one-stage text removal network with both a pre-trained and adversarial network, achieving promising results at a higher resolution.

Inpainting has also been improved by introducing new types of convolution (Liu et al., 2018; Yu et al., 2018a; Iizuka et al., 2017) and multi-stage architectures (Yu et al., 2018a; Nazari et al., 2019). Inspired by these and building upon the work of MTRNet (Tursun et al., 2019), we propose a mask-based one-stage approach for text removal.

3. MTRNet++

MTRNet++ is text-inpainting network, and is formulated as a conditional generative adversarial network Isola et al. (2017). It is composed of a multi-branch generator G and a discriminator D . In the following sections, we illustrate their structures and training strategy.

3.1. Multi-branch Generator

The proposed method is a multi-branch, one-stage text removal approach. As shown in Fig. 2, its generator, G , is composed of three branches: mask-refine G_{MR} , coarse-inpainting G_{CI} , and fine-inpainting G_{FI} branches. All branches have a similar architecture inspired by the network proposed by (Johnson et al., 2016). Each branch has a front-end, a mid-section, and a back-end. The front-end is composed of down-sampling convolutional layers that reduce the image dimensions by a factor of two, while the back-end is a transposed version of the front-end. The mid-section is composed of a set of residual blocks (He et al., 2016). G_{CI} and G_{MR} each have six residual blocks. Their first two residual blocks share weights, while there are attention blocks connecting the last-four residual blocks. As per Nazari et al. (2019), dilated convolutions (Yu and Koltun, 2016) with a dilation factor of two are applied in all residual blocks. MTRNet++, therefore, has a larger receptive field compared to MTRNet, which is important when inpainting text with a large font size. The detailed structures of the aforementioned components are described in Appendix A.

Mask-refine The mask refining process transforms the coarse mask, \mathbf{M} , to a refined mask, \mathbf{M}_r , that only covers text pixels. As shown in Fig. 2, with a concatenation of the input image \mathbf{I} and \mathbf{M} as input, G 's mask refine branch, G_{MR} , generates the refined mask,

$$\mathbf{M}_r = G_{MR}(\mathbf{I}, \mathbf{M}). \quad (1)$$

The objective is to keep dilating a coarse mask such that it covers all text pixels under it. In other words, high recall is expected instead of high precision. To boost the recall, Tversky loss (Salehi et al., 2017), presented in Eq. 2, is introduced as this offers a better trade-off between precision and recall by controlling the weights of false positives and false negatives, which are α and β , in Eq. 2. In experiments, α and β are set to 0.1 and 0.9.

$$\mathcal{L}_{MR} = \frac{\alpha \|\mathbf{M}_r \odot \mathbf{M}_{gt}^c\|_1 + \beta \|\mathbf{M}_r^c \odot \mathbf{M}_{gt}\|_1}{\|\mathbf{M}_r \odot \mathbf{M}_{gt}\|_1 + \alpha \|\mathbf{M}_r \odot \mathbf{M}_{gt}^c\|_1 + \beta \|\mathbf{M}_r^c \odot \mathbf{M}_{gt}\|_1}, \quad (2)$$

where the superscript ‘‘c’’ indicates the inverse of an image, and \odot denotes the Hadamard product.

Data augmentation is applied to the masks during training. We apply two augmentation techniques: *padding* and *filtering*. \mathbf{M} is padded with a random padding factor which is smaller than half of the biggest side of \mathbf{M} . The notation $\mathbf{M}_{p=n}$ represents the padded \mathbf{M} with a padding size n . $\mathbf{M}_{p=0}$ therefore represents the mask generated with ground-truth word/character level bounding box labels. In training, 10% of masks are padded with biggest side of the mask to ensure the model can adapt to the no mask scenario. With random padding, the generator becomes invariant to mask scale. For filtering, 20% of bounding boxes are filtered to keep some text from being removed. Via filtering, generators become aware of mask position and meaning. Note that padding is applied after filtering.

Coarse-inpainting G_{CI} 's coarse-inpainting branch generates a low quality inpainted image,

$$\mathbf{I}_{CI} = G_{CI}(\mathbf{I}, \mathbf{M}_{p=n}), \quad (3)$$

which is used to create a coarse composited image \mathbf{I}_{CI}^c by merging with \mathbf{I} based on \mathbf{M}_r as follows,

$$\mathbf{I}_{CI}^c = \mathbf{M}_r \odot \mathbf{I}_{CI} + (\mathbf{I} - \mathbf{M}_r) \odot \mathbf{I}. \quad (4)$$

Attention blocks Both the mask-refine and coarse-inpainting tasks are focussing on text which needs to be inpainted. G_{MR} is explicitly trained with ground-truth text labels, thus it captures more accurate text position compared to G_{CI} . Here, four attention blocks are applied to transfer text position information to G_{CI} from G_{MR} .

Fine-inpainting G_{FI} utilises both \mathbf{I}_{CI}^c and \mathbf{M}_r as additional auxiliary inputs to generate

$$\mathbf{I}_{FI} = G_{FI}(\mathbf{I}_{CI}^c, \mathbf{M}_r), \quad (5)$$

which is more precise in-painted image and has a more realistic structure in the inpainted area. In the training stage, \mathbf{M}_r is randomly replaced by \mathbf{M}_{gt} . The probability of this replacement decreases from 1 till 0.1 every 2,000 steps in increments of 0.1. We introduce this progressive replacement as the accuracy of \mathbf{M}_r is very low initially and that can impact the convergence of the branch G_{FI} .

Training losses Both coarse-inpainting and fine-inpainting branches are trained with L1, perceptual, style and adversarial losses. These losses are also used in EnsNet, though we introduce some modifications to these losses. Note that style and perceptual losses are calculated based on the last activation maps before the pooling layer after the top five convolution blocks of the VGG-19 network (Simonyan and Zisserman, 2014).

To increase the inpainting quality of text regions covered by masks, weighted L1 loss, weighted style loss and weighted perceptual loss are applied. Weights are assigned based on the input masks. Feature or outputs under masked regions are multiplied by the weight parameter λ . In experiments, λ is empirically set to 10.

The weighted L1 loss \mathcal{L}_1 is defined as

$$\mathcal{L}_1 = \sum_{\mathbf{I} \in \{\mathbf{I}_{CI}, \mathbf{I}_{FI}\}} \mathbb{E}[\|\mathbf{I}_{gt} \odot \mathbf{M}_w - \mathbf{I} \odot \mathbf{M}_w\|_1], \quad (6)$$

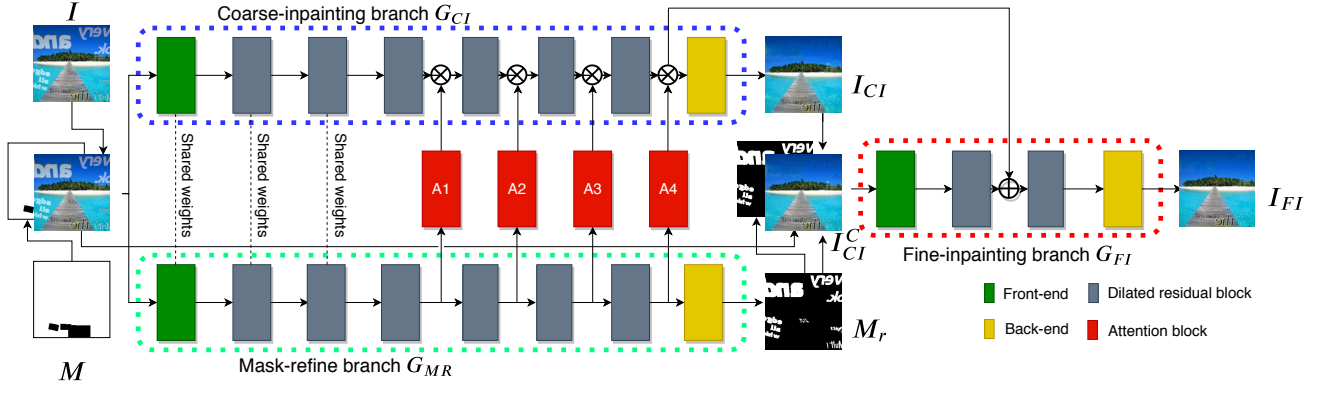


Fig. 2: The overall structure of the proposed one-stage text removal method, MTRNet++. It is composed of mask-refine G_{MR} , coarse-inpainting G_{CI} and fine-inpainting G_{FI} branches. An input to all branches is a channel-wise concatenation of an image and a mask.

where $M_w = \lambda \mathbf{M}_{p=0} + \mathbf{M}_{p=0}^c$.

The weighted perceptual loss \mathcal{L}_{perc} is defined as

$$\mathcal{L}_{perc} = \sum_{\mathbf{I} \in \{\mathbf{I}_{CI}, \mathbf{I}_{RI}\}} \sum_i \frac{1}{N_i} \|\phi_i(\mathbf{I}_{gt}) - \phi_i(\mathbf{I})\|_1, \quad (7)$$

where $\phi_i = \phi_i \odot M_w$, and the notation ϕ_i denotes the activations of the i th convolution block. N_i is the number of activation in layer i .

The weighted style loss is calculated using the Gram matrix of weighted activation maps, ϕ_i , by

$$\mathcal{L}_{style} = \frac{\sum_{\mathbf{I} \in \{\mathbf{I}_{CI}, \mathbf{I}_{RI}\}} \sum_i \|\phi_i(\mathbf{I}_{gt})^T \phi_i(\mathbf{I}_{gt}) - \phi_i(\mathbf{I})^T \phi_i(\mathbf{I})\|_1}{C_i H_i W_i}, \quad (8)$$

where $(H_i W_i) \times C_i$ is the shape of ϕ_i .

In this work, the vanilla adversarial loss is replaced by the hinge loss (Miyato et al., 2018) to enable efficient and stable training. The generator adversarial loss, \mathcal{L}_{adv_G} , is defined as

$$\mathcal{L}_{adv_G} = - \sum_{\mathbf{I} \in \{\mathbf{I}_{CI}, \mathbf{I}_{CI}^c, \mathbf{I}_{RI}, \mathbf{I}_{RI}^c\}} \mathbb{E}[D(\mathbf{M}_{p=0}, \mathbf{I})] \quad (9)$$

The generator G is trained with the loss \mathcal{L}_G ,

$$\mathcal{L}_G = \mathcal{L}_{MR} + \lambda_{L1} \mathcal{L}_{L1} + \lambda_{perc} \mathcal{L}_{perc} + \lambda_{style} \mathcal{L}_{style} + \lambda_{adv_G} \mathcal{L}_{adv_G}, \quad (10)$$

where regularisation parameters λ_{L1} , λ_{perc} , λ_{style} , and λ_{adv_G} are set to 2.5, 0.05, 12.5 and 0.05 in experiments.

3.2. Discriminator

The discriminator is a PatchGAN (Isola et al., 2017) as per MTRNet’s discriminator. However, to implement the network as a Wasserstein GAN (Miyato et al., 2018), spectral normalization is implemented in each layer as per SN-PatchGAN (Yu et al., 2018a). To create a strong discriminator, the original mask $\mathbf{M}_{p=0}$ is concatenated to the input to each of the top four layers to increase attention on the inpainted regions. The detailed structure of the discriminator is provided at Appendix A. The loss for training the discriminator is defined as follow,

$$\begin{aligned} \mathcal{L}_{adv_D} = & \mathbb{E}[\max(\mathbf{0}, 1 - D(\mathbf{M}_{p=0}, \mathbf{I}_{gt}))] \\ & + \sum_{\mathbf{I} \in \{\mathbf{I}_{CI}, \mathbf{I}_{CI}^c, \mathbf{I}_{RI}, \mathbf{I}_{RI}^c\}} \mathbb{E}[\max(\mathbf{0}, 1 + D(\mathbf{M}_{p=0}, \mathbf{I}))], \end{aligned} \quad (11)$$

3.3. Training Setup and Strategy

Our training setup is similar to Edge-connect (Nazeri et al., 2019). PyTorch is used for implementation. All models are trained using 256×256 images with a batch size of eight. The Adam optimiser with $\beta_1 = 0$ and $\beta_2 = 0.9$ is used. The initial learning rate of generator is set to 10^{-4} . It is divided by 10 when the generator loss value stops decreasing. In total, the learning rate is divided by 10 twice. As we used a WGAN, the learning rate of the discriminator is five times that of generator. In large datasets the convergence appears within 200,000 steps, while in small datasets the final convergence appears within 85,000 steps.

4. Experiment

4.1. Datasets and Evaluation Metrics

In this study, MTRNet++ is primarily compared with the previous state-of-the-art methods, MTRNet and EnsNet. For a fair comparison, the same datasets and evaluation metrics introduced by MTRNet and EnsNet are applied. The comparison includes quantitative and qualitative results. Quantitative results are given for synthetic datasets that have ground-truth, while qualitative visualisations are provided for both synthetic and real datasets. Most of the datasets used for training and evaluation are well-known challenging datasets for the text detection task.

Synthetic Datasets The Oxford synthetic real scene text detection (Gupta et al., 2016) and SCUT synthetic text removal (Zhang et al., 2018) datasets are adapted for training and quantitative evaluation. The Oxford dataset includes around 800,000 images. We randomly selected 95% images as training images, 10,000 images as test images, and the rest as validation images. In comparison, the SCUT dataset is a small scale dataset. It

includes 8,000 training images and 800 test images. The Oxford dataset was initially proposed for real scene text detection. It is chosen for demonstrating the robustness of MTRNet++. In comparison, the SCUT dataset is selected as it was built for text removal and it includes some real cases. Its background images are manually modified images from the ICDAR 2013 (Karatzas et al., 2013) and ICDAR 2017 MLT (Nayef et al., 2017) datasets.

Synthetic Refined Mask MTRNet++ is a mask-based method. It not only uses masks generated by ground-truth word/character-level polygonal bounding boxes, but also requires pixel-level ground-truth masks for the mask-refining task. However, ground-truth refined masks are not provided by Oxford or SCUT datasets. We created ground-truth refined masks based on the pixel value differences between input and ground-truth images. We assume that input and its ground-truth have pixel value differences only on text pixels. To avoid noise, we used a threshold set to 25. Moreover, we also suppress noise in non-text regions based on the word/character level bounding boxes.

Evaluation Metrics In previous studies (Nakamura et al., 2017; Zhang et al., 2018; Tursun et al., 2019), text removal methods are evaluated with text detectability and inpainting quality. Nakamura et al. (2017) assumes that a high quality text removal method will decrease text detectability. To this end, a robust text detection method is applied to text inpainted images, and precision and recall values are calculated. Precision and recall values are expected to be zero after successful text removal. Zhang et al. (2018) introduced evaluation metrics widely used in inpainting to evaluate the quality of the inpainting. They found the quality of the inpainting can't be captured by the precision or recall scores. To evaluate the quality or realistic degree of inpainting, PSNR, SSIM, MSE and MAE scores are calculated when the ground truth images are available. Note that, for text detection, we applied the recent state-of-the-art text detection method CRAFT (Baek et al., 2019), and for evaluation the DetEval (Wolf et al., 2014) protocol is used.

4.2. Outputs of MTRNet++

MTRNet++'s three branches output a refined-mask, a coarse-inpainted image and a fine-inpainted image for a given input. In this work, these coarse and fine predicted images are referred to as *predicted*. These predicted results are further improved via replacing non-text regions with the corresponding regions in the given input based on the refined-mask. The resultant composited images are referred to as *composited*. We found colour discontinuities appear near the text boundary on composited images. Although they are very subtle discontinuities, text can be recognisable as text. To overcome colour discontinuities, a dilatation operation with a disk of radius seven is applied to the refined-mask before the composition. The dilatation operation not only reshapes the boundaries but also shifts boundaries to regions with fewer colour discontinuities. The composited fine-inpainting results are used when MTRNet++ is compared with other methods as these represent the best output of the network.

4.3. Comparison with State-of-the-Art

MTRNet++ is compared with the previous state-of-the-art one-stage (EnsNet, Pix2Pix) and two-stage (MTRNet) approaches on both Oxford and SCUT datasets. In the following section, we will discuss and analyse their results, but before that we briefly introduce their implementation details:

- We trained MTRNet++ on both Oxford and SCUT training datasets with the training setup and strategy provided in Section 3.3. MTRNet++ is trained for 200,000 steps on the Oxford training set, and for 85,000 steps on the SCUT training set. For a fair comparison, when MTRNet++ is compared with other state-of-the-art methods, full coarse masks were provided.
- We reimplemented EnsNet with the same settings as MTRNet++ by replacing MTRNet++'s generator with EnsNet's generator. We trained EnsNet on both SCUT and Oxford datasets in the same way that MTRNet++ was trained. We ensure that the reimplemented EnsNet achieves comparable results on the SCUT test set with those reported by Zhang et al. (2018). As no public EnsNet trained model is available, we used the results of the reimplemented EnsNet for all visual comparisons.
- We tested Pix2Pix and MTRNet using the models trained by Tursun et al. (2019). Both were trained for 300,000 steps with a batch size 16. Note that word-level ground-truth bounding box masks were provided for MTRNet.

Quantitative results of the comparison on Oxford and SCUT test sets are given in Table 1 and 2 respectively. Inpainting quality related scores are provided for both Oxford and SCUT datasets, while text detection related scores are only provided for the Oxford dataset as the SCUT dataset's relevant ground-truth is not publicly available yet. Qualitative comparisons are given in Figs. 3 and 4.

MTRNet++ achieved the highest PSNR and SSIM and lowest MSE scores on the Oxford test set by a large margin. It also achieved the second-best performance on the adversarial text detection evaluation with a marginal difference between it and MTRNet, even though MTRNet++ used coarse masks while MTRNet used ground-truth masks. The qualitative results in Fig. 3 show that MTRNet++'s inpainting results are close to the ground-truth, while the results of MTRNet and EnsNet are blurry. What's more, EnsNet's results are also incomplete and partially damaged.

MTRNet++ also achieved comparable inpainting results on the SCUT dataset when compared to the previous state-of-the-art results reported by Zhang et al. (2018), while it slightly surpassed the reimplemented EnsNet. In Fig. 4, the results of MTRNet++ and EnsNet are close to the ground-truth, while MTRNet's results are blurry and incomplete.

One of the reasons EnsNet's results are comparable to MTRNet++ on a small-scale dataset and not on a large scale dataset is that it lacks good generalisation. We believe that EnsNet memorises the ground-truth in the SCUT dataset as it only has 1,223 ground-truth backgrounds for 8,000 training images. However, MTRNet++ is difficult to overfit even on a small dataset for two

reasons: 1. The refined-mask branch output is unique for each input, even though some inputs share the same background, as it predicts text masks on the foreground. 2. The two types of augmentation, padding and filtering, introduced in Section 3 create a new background for each input image.

In summary, MTRNet++ achieved the state-of-the-art results on both Oxford and SCUT datasets. MTRNet++’s results are complete, realistic and stable.

4.4. Ablation Studies

Fine-inpainting Branch We studied the importance of the fine-inpainting branch by providing composited and predicted coarse and fine inpainting results. Those results for Oxford and SCUT datasets are given in Tables 3 and 4. On both datasets the composited fine-inpainting achieved the best results, and has surpassed the predicted coarse-inpainting results by a large margin. In Fig. 5, the composited fine-inpainting has less artifacts than the coarse-inpainted version. Both qualitative and quantitative results show the fine-inpainting branch is beneficial for more realistic inpainting.

Mask-Refine Branch To prove the importance of the mask-refine branch, an MTRNet++ without the mask-refine branch is trained in the same manner as MTRNet++. The related quantitative comparison on the Oxford test set is provided in Table 5. MTRNet++ surpassed its no mask-refine branch variant in PSNR, SSIM and MAE scores by a large margin. Moreover, the mask-refine branch is also robust to very coarse masks. For example, MTRNet++’s scores decrease less than its variant when the mask padding is increased in Table 5. Similar results are also found in Tables 1 and 2 where MTRNet++ is less negatively affected by the degree of coarseness of the masks thanks to the mask-refine branch. The mask-refine branch therefore is essential for MTRNet++.

Mask-Refine Loss We used Tversky loss as the mask-refine loss to ensure a high recall value. From Table 1 and 2, we can see that MTRNet++ achieved very high recall values with high precision values. For example, MTRNet++ achieved at least 97% recall on both Oxford and Synthetic datasets.

Attention Block To test the role of attention blocks in MTRNet++, we trained an MTRNet++ variant without attention blocks. From Table 5, we can see that MTRNet++’s performance declines when attention blocks are missing. We also visualised the activations of the four attention blocks of the generator of MTRNet++ for randomly selected images in Fig. 6. Low-level attention blocks, A1 and A2, show high activations on text regions, while high-level attention blocks, A3 and A4, have low activations on text regions. Especially, the attention block A4 assigns the lowest attention to text regions. All those results show that attention blocks are beneficial for MTRNet++.

4.5. Controllability and Interpretability

Selective Text Removal As shown in Fig. 7, MTRNet++ is able to selectively remove text via designing the masks. MTRNet++ only erases text under the given masks, and only generates refined masks for text that needs to be removed.

Interpretability Interpretability is important for diagnosing failure cases. MTRNet++’s intermediate results help analysing

failure cases. For example, two failure cases are given in Fig. 8. The reason for the first case (top row) is related to inpainting branches since the predicted mask is accurate. In comparison, the second case (bottom row) is related to mask-refine branch as the mask is not complete.

5. Conclusion

In this work, a one-stage mask-based conditional generative adversarial network, MTRNet++, is proposed for real-scene text removal. It is self-complete, controllable and interpretable. It shows state-of-the-art quantitative results on both the Oxford and SCUT test datasets without user-provided text masks. Visual results also show MTRNet++ generates realistic inpainting for text regions. Related ablation studies show that proposed multi-branch generator is essential for state-of-the-art performance. Moreover, MTRNet++ is easily trainable in an end-to-end way. MTRNet++ converges on a large-scale dataset within an epoch. MTRNet++ also shows its controllability and interpretability.

Acknowledgements

This research was supported by an Advance Queensland Research Fellowship Award.

References

- Baek, Y., Lee, B., Han, D., Yun, S., Lee, H., 2019. Character region awareness for text detection, in: Proceedings of the IEEE Conference on Computer Vision and Pattern Recognition, pp. 9365–9374.
- Gupta, A., Vedaldi, A., Zisserman, A., 2016. Synthetic data for text localisation in natural images, in: Proc. of CVPR.
- He, K., Zhang, X., Ren, S., Sun, J., 2016. Deep residual learning for image recognition, in: Proceedings of the IEEE conference on computer vision and pattern recognition, pp. 770–778.
- Iizuka, S., Simo-Serra, E., Ishikawa, H., 2017. Globally and locally consistent image completion. ToG.
- Isola, P., Zhu, J.Y., Zhou, T., Efros, A.A., 2017. Image-to-image translation with conditional adversarial networks. CVPR.
- Jo, Y., Park, J., 2019. Sc-fegan: Face editing generative adversarial network with user’s sketch and color. arXiv preprint arXiv:1902.06838.
- Johnson, J., Alahi, A., Fei-Fei, L., 2016. Perceptual losses for real-time style transfer and super-resolution, in: ECCV.
- Karatzas, D., Shafait, F., Uchida, S., Iwamura, M., Bigorda, L.G., Mestre, S.R., Mas, J., Mota, D.F., Almazan, J.A., De Las Heras, L.P., 2013. Icdar 2013 robust reading competition, in: ICDAR.
- Khodadadi, M., Behrad, A., 2012. Text localization, extraction and inpainting in color images, in: 2012 20th Iranian Conf. on Electrical Engineering (ICEE), pp. 1035–1040.
- Liu, G., Reda, F.A., Shih, K.J., Wang, T.C., Tao, A., Catanzaro, B., 2018. Image inpainting for irregular holes using partial convolutions, in: Proc. of ECCV, pp. 85–100.
- Ma, Y., Liu, X., Bai, S., Wang, L., He, D., Liu, A., 2019. Coarse-to-fine image inpainting via region-wise convolutions and non-local correlation, in: Proceedings of the 28th International Joint Conference on Artificial Intelligence, AAAI Press. pp. 3123–3129.
- Maas, A.L., Hannun, A.Y., Ng, A.Y., 2013. Rectifier nonlinearities improve neural network acoustic models, in: Proc. icml, p. 3.
- Mao, X.J., Shen, C., Yang, Y.B., 2016. Image restoration using convolutional auto-encoders with symmetric skip connections. arXiv preprint arXiv:1606.08921.
- Miyato, T., Kataoka, T., Koyama, M., Yoshida, Y., 2018. Spectral normalization for generative adversarial networks. arXiv preprint arXiv:1802.05957.

Table 1: The results of a comparison on the test set of the Oxford Synthetic dataset.

Method	PSNR	SSIM(%)	MSE (%)	Precision (%)	Recall (%)	F-score
Original images	-	-	-	76.41	44.27	56.06
Pix2Pix (Isola et al., 2017)	24.63	89.73	0.54	70.03	29.34	41.35
MTRNet (Tursun et al., 2019)	28.99	93.18	0.20	35.83	0.26	0.52
EnsNet (Zhang et al., 2018)	27.42	94.37	0.21	57.25	14.34	22.94
MTRNet++	33.67	98.43	0.05	50.43	1.35	2.63

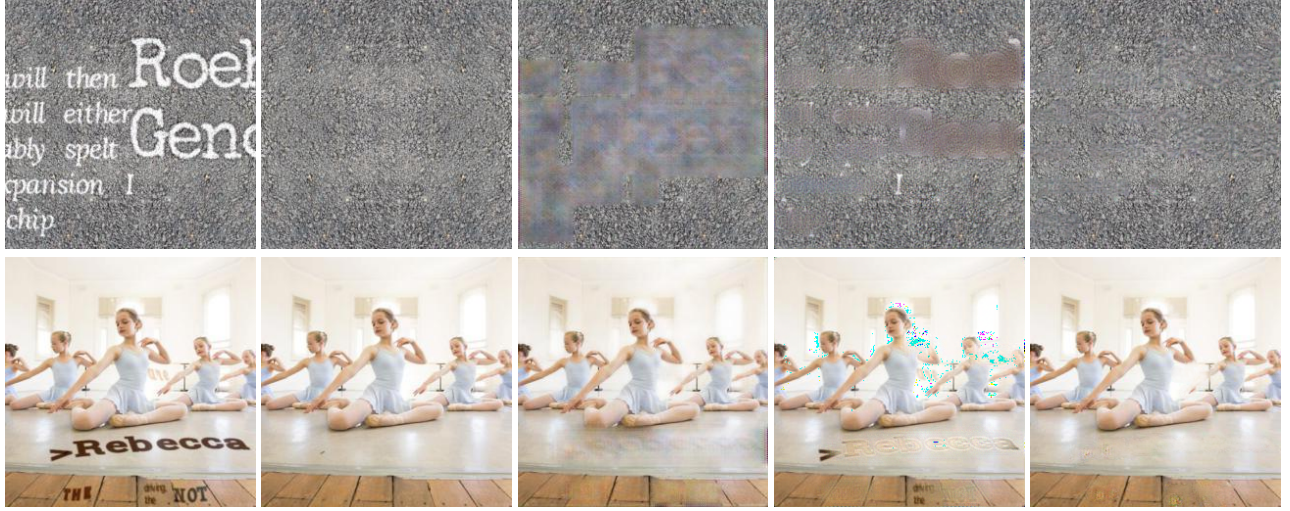


Fig. 3: Visual comparison of text removal methods on the Oxford test set. From left to right, input, ground truth, MTRNet, EnsNet and MTRNet++.

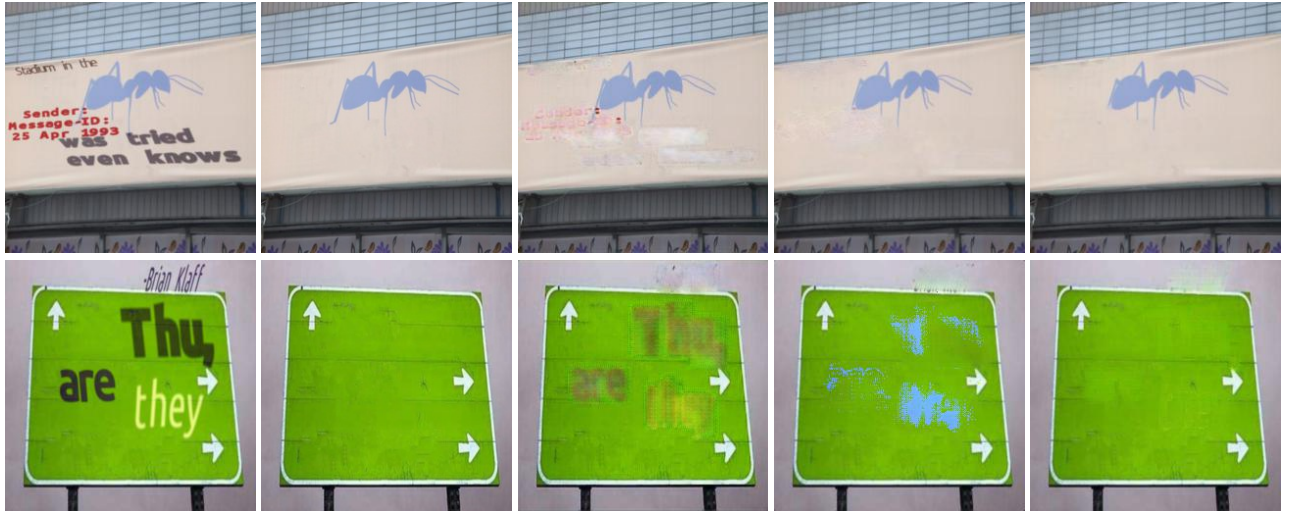


Fig. 4: Visual comparison of text removal methods on the SCUT test set. From left to right, input, ground truth, MTRNet, EnsNet and MTRNet++.

Table 2: Comparison on the test set of the SCUT dataset.

Method	PSNR	SSIM(%)	MSE (%)
Pix2Pix (Isola et al., 2017)	25.60	89.86	24.56
STE (Nakamura et al., 2017)	14.68	46.13	71.48
MTRNet (Tursun et al., 2019)	29.71	94.43	0.01
EnsNet (Zhang et al., 2018)	37.36	96.44	0.20
EnsNet (Reimplemented)	34.16	98.10	0.04
MTRNet++	34.55	98.45	0.04

- Nakamura, T., Zhu, A., Yanai, K., Uchida, S., 2017. Scene text eraser, in: ICDAR, pp. 832–837.
- Nayef, N., Yin, F., Bizid, I., Choi, H., Feng, Y., Karatzas, D., Luo, Z., Pal, U., Rigaud, C., Chazalon, J., et al., 2017. Icdar2017 robust reading challenge on multi-lingual scene text detection and script identification-rrc-mlt, in: ICDAR, pp. 1454–1459.
- Nazeri, K., Ng, E., Joseph, T., Qureshi, F., Ebrahimi, M., 2019. Edgeconnect: Generative image inpainting with adversarial edge learning. arXiv preprint arXiv:1901.00212 .
- Salehi, S.S.M., Erdogmus, D., Gholipour, A., 2017. Tversky loss function for image segmentation using 3d fully convolutional deep networks, in: Int. Workshop on MLMI, Springer.
- Simonyan, K., Zisserman, A., 2014. Very deep convolutional networks for

Table 3: Evaluation of MTRNet++ with various scale masks on the test set of the Oxford dataset. Precision and Recall of refined-masks are calculated for the mask-refine branch. PSNR, SSIM, MAE values are calculated for predicted and composited images from both the coarse-inpainting and fine-inpainting branches.

Pad	Mask-Refine			Type	Coarse-inpainting			Fine-inpainting		
	Precision (%)	Recall (%)	F1		PSNR	SSIM (%)	MAE (%)	PSNR	SSIM (%)	MAE (%)
0	82.80	97.74	89.65	predicted	29.31	95.76	5.03	32.69	97.56	3.06
				composited	35.19	98.46	0.77	35.88	98.52	0.69
100	76.76	97.15	85.76	predicted	28.95	95.66	5.12	31.96	97.47	3.13
				composited	34.42	98.47	0.82	34.56	98.50	0.78
256	72.92	97.01	83.26	predicted	28.69	95.63	5.19	31.43	97.41	3.20
				composited	33.87	98.43	0.87	33.67	98.43	0.85

Table 4: Evaluation of MTRNet++ with various scale masks on the test set of the SCUT dataset. Precision and Recall of refined-masks are calculated for the mask-refine branch. PSNR, SSIM, MAE values are calculated for predicted and composited images from both the coarse-inpainting and fine-inpainting branches.

Pad	Mask-Refine			Type	Coarse-inpainting			Fine-inpainting		
	Precision (%)	Recall (%)	F1		PSNR	SSIM (%)	MAE (%)	PSNR	SSIM (%)	MAE (%)
0	88.23	97.97	92.85	predicted	30.67	95.90	3.53	33.18	97.48	2.50
				composited	34.11	98.37	0.77	35.48	98.51	0.65
100	81.53	97.92	88.98	predicted	30.35	95.83	3.58	32.60	97.37	2.55
				composited	33.61	98.43	0.82	34.68	98.55	0.70
256	80.51	97.93	88.37	predicted	30.27	95.83	3.60	32.50	97.35	2.56
				composited	33.50	98.42	0.83	34.55	98.54	0.71

Table 5: Comparison of the variants of MTRNet++ on the Oxford Synthetic test. Here, MTRNet++ is compared with its no mask-refine branch and no attention block variants.

Pad	MTRNet++			MTNet++ without mask-refine			MTNet++ without attention		
	PSNR	SSIM (%)	MAE (%)	PSNR	SSIM (%)	MAE (%)	PSNR	SSIM (%)	MAE (%)
0	35.48	98.51	0.65	26.94	93.44	6.37	33.18	98.31	0.91
50	34.73	98.57	0.69	25.94	92.40	6.82	32.43	98.31	0.99
100	34.68	98.55	0.70	25.38	91.87	7.26	32.04	98.28	1.03
150	34.67	98.55	0.70	24.94	91.53	7.73	31.88	98.26	1.05
256	34.55	98.54	0.71	24.46	91.21	8.34	31.71	98.24	1.07



Fig. 5: Visual comparison of coarse and fine outputs of MTRNet++. From left to right, input, ground truth, coarse inpaint and fine inpaint.

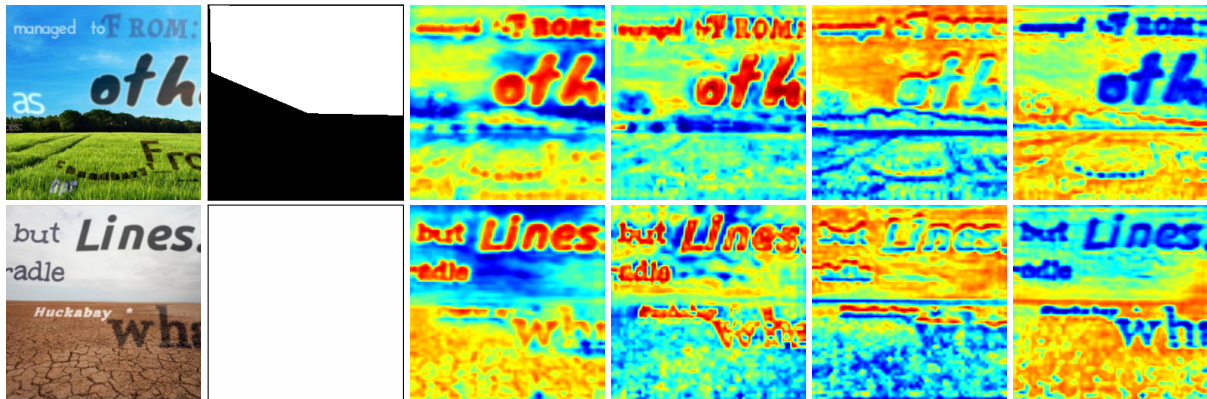


Fig. 6: Example visualisations of the activations of the attention blocks. From left to right, input, mask, attention blocks: A1, A2, A3 and A4.

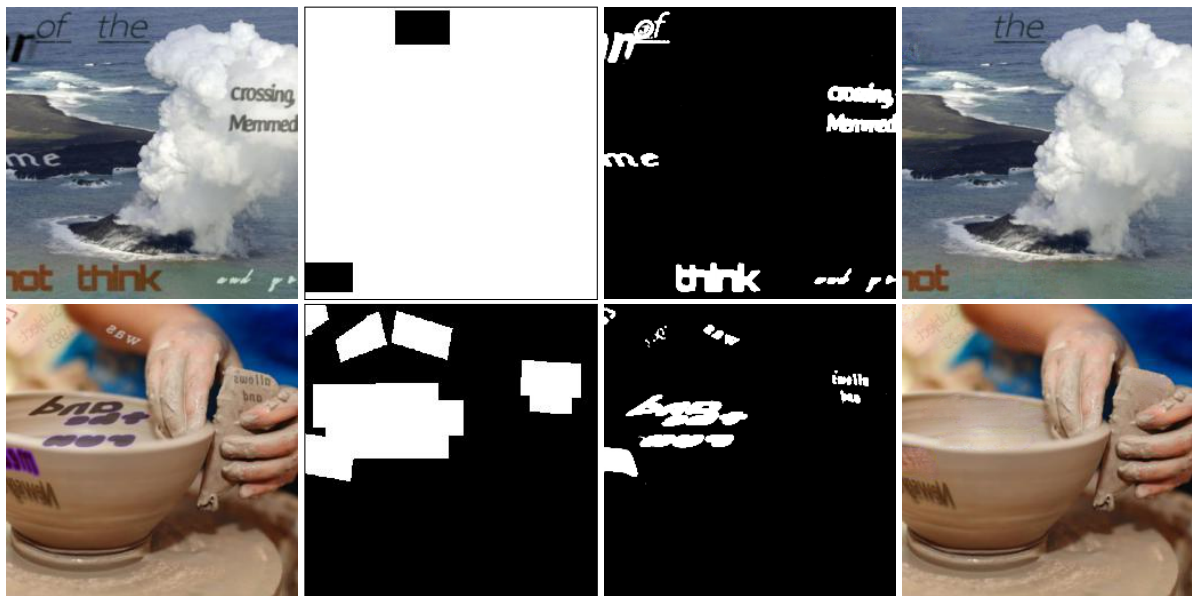


Fig. 7: Examples of partial text removal. First and second columns show the inputs; Third and fourth columns are outputs of MTRNet++.



Fig. 8: Examples of interpretability. From left to right, input, predicted mask and predicted image.

Tursun, O., Zeng, R., Denman, S., Sivipalan, S., Sridharan, S., Fookes, C.,
2019. Mtrnet: A generic scene text eraser. ICDAR .
Ulyanov, D., Vedaldi, A., Lempitsky, V., 2017. Improved texture networks:

Maximizing quality and diversity in feed-forward stylization and texture
synthesis, in: Proc. of CVPR, pp. 6924–6932.
Wagh, P.D., Patil, D., 2015. Text detection and removal from image using

- inpainting with smoothing, in: 2015 Int. Conf. on Pervasive Computing (ICPC), pp. 1–4.
- Wolf, C., Lombardi, E., Mille, J., Celiktutan, O., Jiu, M., Dogan, E., Eren, G., Baccouche, M., Dellandrea, E., Bichot, C.E., et al., 2014. Evaluation of video activity localizations integrating quality and quantity measurements. *Computer Vision and Image Understanding (CVIU)* 127, 14–30.
- Yang, C., Lu, X., Lin, Z., Shechtman, E., Wang, O., Li, H., 2017. High-resolution image inpainting using multi-scale neural patch synthesis, in: *Proc. of the CVPR*.
- Yu, F., Koltun, V., 2015. Multi-scale context aggregation by dilated convolutions. *arXiv preprint arXiv:1511.07122*.
- Yu, F., Koltun, V., 2016. Multi-scale context aggregation by dilated convolutions, in: *ICLR*.
- Yu, J., Lin, Z., Yang, J., Shen, X., Lu, X., Huang, T.S., 2018a. Free-form image inpainting with gated convolution. *arXiv preprint arXiv:1806.03589*.
- Yu, J., Lin, Z., Yang, J., Shen, X., Lu, X., Huang, T.S., 2018b. Generative image inpainting with contextual attention. *arXiv preprint arXiv:1801.07892*.
- Zhang, S., Liu, Y., Jin, L., Huang, Y., Lai, S., 2018. Ensnet: Ensconce text in the wild. *arXiv preprint arXiv:1812.00723*.

Appendix A. Generator and Discriminator Architectures

Notations described in Table A.6 will be used for describing the structure of generator and discriminator. The generator architecture is given in Fig. 2. The generator repeatedly uses several component blocks whose structures are show in Table A.7. The structure of the discriminator is as follow:

64c4p1s2-SP-LRL, MC-128c4p1s2-SP-LRL, MC-256c4p1s2-SP-LRL, MC-512c4p1s1-SP-LRL, MC-1c4p1s1-SP

Table A.6: The notation and their explanation used for describing the network architecture.

Not.	Translation	Usage
c	2D convolution	mc_n is $n \times n$ convolution with m filters.
s	2D convolution stride	sn is a stride with step size n . The default step size is 1.
p	2D convolution padding	pn is a padding with size n . The default padding size is 0.
d	2D convolution dilation Yu and Koltun (2015)	dn is a dilation with size n . The default dilation size is 1.
RP	Reflection padding	RP_n is a reflection padding with the size of n .
IN	Instance normalisation Ulyanov et al. (2017)	
SP	Spectral normalisation Miyato et al. (2018)	
RC	Residual connection He et al. (2016)	
MC	Mask concatenation	the MC operation concatenates the input mask to the previous layer output. The mask is resized to the previous layer output size via nearest neighbour resize.
RL	Relu	
S	Sigmoid	
LRL	Leaky relu (Maas et al., 2013)	LeakyReLU is employed with slope 0.2.

Table A.7: The detailed structure of components of the generator.

Component	Structure
Front-end	RP3-64c4p1s2-IN-RL, 128c4p1s2-IN-RL, 128c4p1s2-IN-RL
Back-end (Inpaint branch)	256u4p1s2-IN-RL, 128c4p1s2-IN-RL, RP3-3c7
Back-end (Mask-refine branch)	256u4p1s2-IN-RL, 128c4p1s2-IN-RL, RP3-1c7
Residual block	RP2-256c3d2-IN-RL, RP1-256c3-IN-RC
Attention block	RP1-128c3-IN-RL, RP1-1c3-IN-S